A Decentralized Adaptive Control Method for Frequency Regulation and Power Sharing in Autonomous Microgrids

Heydari, Rasool; Khayat, Yousef; Naderi, Mobin; Anvari-Moghaddam, Amjad; Dragicevic, Tomislav; Blaabjerg, Frede

Published in:
Proceedings of 2019 IEEE 28th International Symposium on Industrial Electronics (ISIE)

DOI (link to publication from Publisher):
10.1109/ISIE.2019.8781102

Publication date:
2019

Document Version
Accepted author manuscript, peer reviewed version

A Decentralized Adaptive Control Method for Frequency Regulation and Power Sharing in Autonomous Microgrids

Rasool Heydari
Department of Energy Technology
Aalborg University, Denmark
RAH@et.aau.dk

Yousef Khayat
Department of Energy Technology
Aalborg University, Denmark
YKH@et.aau.dk

Mobin Naderi
Department of Energy Technology
Aalborg University
MOb@et.aau.dk

Amjad Anvari-Moghaddam
Department of Energy Technology
Aalborg University, Denmark
AMM@et.aau.dk

Tomislav Dragicevic
Department of Energy Technology
Aalborg University, Denmark
TDR@et.aau.dk

Frede Blaabjerg
Department of Energy Technology
Aalborg University, Denmark
FBL@et.aau.dk

***Abstract*—In this paper, a novel decentralized control structure is proposed to compensate voltage and frequency deviations of an ac microgrid (MG) with higher bandwidth compared to the conventional control structure with no need for a communication network. This approach is realized by firstly employing finite control set model predictive control of voltage source converter at the primary control level. Then, an adaptive droop control is presented to keep the voltage and frequency of the MG stable in steady state and serve as a secondary level of hierarchical control. Therefore, the MG voltage and frequency are restored to the nominal value with a decentralized communication-free control structure. Simulation results verify the accurate frequency and voltage restoration as well as fast power-sharing during the transient and steady-state performance with no need for communication infrastructure.**

***Index Terms*—Adaptive droop, frequency control, power sharing, microgrid, model predictive control.**

I. Introduction

Control objective of a microgrid (MG) is accomplished by utilizing a hierarchical control structure to set the system voltage and frequency on the desired value. Hierarchical control architecture comprises primary, secondary and finally tertiary control level. These control layers differ in terms of bandwidth, dynamic response time and the communication infrastructure requirements. The first layer controls the frequency and voltage locally with the highest bandwidth. Primary control should be able to react very fast and keep the voltage and frequency stable during the load changes. Conventional primary control loop compensates for voltage and frequency deviations in order of several seconds [1], [2]. In this hierarchical structure, the secondary controller should be designed to compensate for the steady state errors caused by primary control level. Obviously, the secondary control level should be implemented with lower bandwidth compared to the inner primary level in order to avoid the undesired interactions of control loops. Optimal operation of distributed generations (DGs), plug in/out of each unit and long term operation issues such as economic dispatch are determined in the tertiary control level which also called global controller [3]–[6].

It worth to note that, the primary control level is generally distributed, while tertiary control is a centralized control level. However, secondary control level is introduced in the literature to be operated in centralized [7]–[9], distributed [10]–[13] and totally decentralized manner [14]–[17]. In the centralized structure, in order to achieve comprehensive controllability, each DG sends the required data (frequency and voltage amplitude) to a central controller (MGCC), then, MGCC sends a compensatory signal to each DG to change its droop set-point and compensate for frequency and voltage deviations. The main advantage of this structure is the strong observability and controllability of the whole system. However, in the centralized structure, the secondary control performance is highly depended on the communication network and central controller. Therefore, any failure in the communication network or MGCC degrade the performance of secondary control and decrease the system reliability [8], [18]. In order to overcome the aforementioned problem distributed control framework has been presented [12], [19]. This structure uses the advanced communication algorithms such as (consensus, peer to peer and Open FMB) for sharing the required data with minimum bandwidth. Secondary control is implemented locally like the primary control level, and communication link at the upper level share the required data among DGs. This approach enhances the reliability of the system by minimizing the transmitted data, hence, decreasing the dependency to the communication link and also the central controller. However, this coordinated performance make the system more complex to design, while the communication network is still needed. The fully decentralized control architecture of secondary control is based on the local measurement and estimation. In this

structure, secondary control is implemented locally, and by using the individual local states and estimating the neighbour variables, provide the adjustment signal for primary control. In this paper, a novel decentralized control structure based on the adaptive droop control is proposed. The major contribution of this paper is as follows:

1) By applying advanced control structure at the primary control level and also decentralized adjusting the droop set point, higher bandwidth operation of the MG is achieved. Thus, the MG frequency and voltage are compensated much faster than conventional methods presented in the literature.

2) Compared to the conventional control structures, the proposed decentralized approach enhances the MG reliability by employing a communication-free structure and lack of communication network failures.

II. Conventional Control Structure

Power electronic based MG consists of several paralleled grid supporting VSCs, which exchange power with ac bus and regulate the MG voltage and frequency. In order to have a comprehensive controllablity, a hierarchical control structure is employed. Local primary control in the lowest level regulates the output voltage of the converter, while the upper level secondary control compensates for voltage and frequency deviations in steady state.

A. Primary control level

Local voltage and frequency regulation, as well as active and reactive power sharing among DGs are carried out in the primary control level. The independent inner control loops and also droop control compose the infrastructure of the primary control level.

1) Inner loops: Conventionally, current and voltage control loops are utilized in primary control level to stabilize the output voltage and frequency of the VSCs. Proportional resonant controllers in $\alpha\beta$ frame and proportional integral (PI) controllers in dq frame are mostly used in inner control loops. However, in order to avoid undesirable interaction in the control structure, outer loops should be designed in lower bandwidth compared to the inner loops. More details about inner voltage and current loops are addressed in [18]

As an alternative solution, single loop primary control methods such as finite control set MPC (FCS-MPC) or robust control methods by stabilizing the current and voltage of the VSC in a cost function is presented in [20].

The main idea of these control structure is to substitute both inner voltage and current control loops with a predictive based single controller. In this control structure, an applicable gating signal can be selected based on the system model and predefined cost function minimization.

Considering a simple two level three phase VSC, with three main gating signals. Its voltage output can be controlled by choosing the appropriate switching configuration, shown in Table I.

Switching states of the two-level tree-phase VSC can be achieved by three binary gating signals i.e. S_a, S_b, and S_c. By applying the complex Clarke transformation, eight (2^3) switching configuration are possible. The corresponding voltage vectors v_i in the complex $\alpha-\beta$ frame are shown in Table I. The FCS-MPC control strategy is based on the output voltage prediction and adapts appropriate input signals so that the output voltage follows the reference voltage trajectory. Therefore, the CF is the error between the predicted output voltage and reference voltage. Then, the corresponding input vector with minimum CF is applied to the VSC. One of the main merits of this control strategy is that by adapting the CF all required constraints can be achieved. Thus, in this paper three terms are added to the CF. 1) Current constraint. 2) Switching effort. 3) Voltage derivative error. The third term is added to decrease the total harmonic distortion (THD) [20]. Therefore, the overall CF can be formulated as follows:

TABLE I. Two Level Three Phase VSC Switching States.

Voltage vector $\overline{v}_i$	S_a	S_b	S_c
$\overline{v}_0 = 0$	0	0	0
$\overline{v}_1 = \frac{2}{3}v_{dc}$	1	0	0
$\overline{v}_2 = \frac{1}{3}v_{dc} + j\frac{\sqrt{3}}{3}v_{dc}$	1	1	0
$\overline{v}_3 = -\frac{1}{3}v_{dc} + j\frac{\sqrt{3}}{3}v_{dc}$	0	1	0
$\overline{v}_4 = -\frac{2}{3}v_{dc}$	0	1	1
$\overline{v}_5 = -\frac{1}{3}v_{dc} - j\frac{\sqrt{3}}{3}v_{dc}$	0	0	1
$\overline{v}_6 = \frac{1}{3}v_{dc} - j\frac{\sqrt{3}}{3}v_{dc}$	1	0	1
$\overline{v}_7 = 0$	1	1	1

$$CF : \|\overline{v}_e(i)\|^2 + \xi_{lim}(i) + \zeta_w SW^2(i)) + G_d, \tag{1}$$

$$\overline{v}_e(i) = \overline{v}^*_f(i) - \overline{v}_e(i), \tag{2}$$

$$\xi_{lim}(i) = \begin{cases} 1, & \text{if } |i_f(i)| \leq i_{max} \\ \infty, & \text{if } |i_f(i)| > i_{max} \end{cases}, \tag{3}$$

$$SW(i) = \sum |u(i) - u(i-1)|, \tag{4}$$

$$G_d = \left(\frac{d\overline{v}^*_f(t)}{dt} - \frac{d\overline{v}_f(t)}{dt}\right) = (C_f\omega_{ref}v^*_{f\beta} - i_{f\alpha} + i_{o\alpha})^2 + (C_f\omega_{ref}v^*_{f\alpha} - i_{f\beta} + i_{o\beta})^2 \tag{5}$$

Where $v_e(i)$ represents the output prediction error, $\overline{v}^*_f(i)$ is the reference voltage and $\overline{v}_e(i)$ is the predicted output voltage. Furthermore, $\xi_{lim}(i)$ represents the current constraint, $SW(i)$ is switching effort with a weighting factor ζ_w and G_d exposes the derivative error. The reference voltage is determined through droop control and virtual impedance in the upper level.

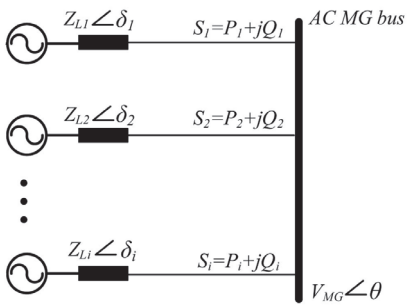

Fig. 1. Simplified model of VSCs connected to ac MG bus with loads.

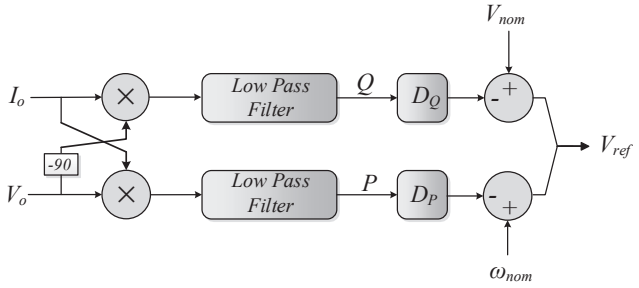

Fig. 2. Droop control diagram for the inductive output impedance in a MG.

2) Droop control and virtual impedance: Power control and active/reactive power sharing in the primary control level can be achieved by utilizing a droop control strategy. The foundation of VSC-based MG is illustrated in Fig. 1. The equation that defines the principles of power exchange (active and reactive) between the VSC and ac bus is as follows:

$$V_{MG}I_i^* = \frac{V_{MG}V_i\angle\theta - \delta_i}{Z_{L_i}} - \frac{V_{MG}^2\angle\theta}{Z_{L_i}}. \tag{6}$$

By neglecting the high-frequency harmonics, VSC behaves as an ac source with an amplitude of V_i and power angle of δ_i, while MG bus voltage is $V_{MG}\angle 0$ and connection impedance is $Z_{L_i}\angle\theta_i$. Thus, the exchanged active and reactive power can be obtained as:

$$P = \frac{V_{MG}V_i}{Z_{L_i}}\cos(\theta-\delta_i) - \frac{V_{MG}^2}{Z_{L_i}}cos(\theta), \tag{7}$$

$$Q = \frac{V_{MG}V_i}{Z_{L_i}}\sin(\theta-\delta_i) - \frac{V_{MG}^2}{Z_{L_i}}sin(\theta_i). \tag{8}$$

It can be demonstrated from (7) and (8) that power exchange relies on both voltage and power angle of VSC. To control the power by those variables independently, virtual impedance concept is commonly used [21]. By applying virtual impedance, the output impedance, seen by the VSC, can be enforced to be either purely inductive or resistive. If the output impedance is considered as a purely inductive ($\theta_i = 90$) or purely resistive ($\theta_i = 0$) and also the phase difference between VSC voltage vector and MG bus voltage is assumed small enough to state that $cos(\delta) = 1$, and $sin(\delta) = \delta$, then (7) and (8) can be simplified to:

$$\begin{cases} P = \dfrac{V_{MG}V_i}{Z_L}\delta_i \\ Q = \dfrac{V_{MG}V_i - V_{MG}^2}{Z_{L_i}} \end{cases} \text{for inductive output impedance,} \tag{9}$$

$$\begin{cases} P = \dfrac{V_{MG}}{R_{L_i}}.(V_i - V_{MG}) \\ Q = \dfrac{-V_{MG}V_i}{R_{L_i}}.\dfrac{\omega_i}{s} \end{cases} \text{for resistive output impedance.} \tag{10}$$

Thus, in such a system active and reactive power exchange can be controlled independently, based on the droop control characteristics, which are shown in Fig. 2 and formulated as follows:

$$\begin{cases} \omega_{ref} = \omega_{nom} - D_P P \\ V_{ref} = V_{nom} - D_Q Q \end{cases} \text{for inductive output impedance,} \tag{11}$$

$$\begin{cases} \omega_{ref} = \omega_{nom} + D_Q Q \\ V_{ref} = V_{nom} - D_P P \end{cases} \text{for resistive output impedance.} \tag{12}$$

where ω_{ref} and V_{ref} refer to reference frequency and voltage amplitude respectively, whereas, ω_{nom} and V_{nom} are nominal frequency and voltage amplitude of VSC at no load, correspondingly. At upper level, secondary control is required to compensate for frequency and voltage deviations in steady state. Conventionally, secondary control comprises a central controller (MGCC) and low bandwidth communication infrastructure. The MG voltage amplitude and frequency are compared with a reference value and then compensatory signals are sent to each DG through the communication link. The main drawback of the conventional secondary control structure is that any failure in communication link or MGCC leads to the collapse in secondary control level and maybe instability in the voltage or frequency of the MG.

III. Proposed adaptive droop control

In order to overcome the aforementioned challenge, a new distributed control structure is proposed. In this structure, an adaptive control term is added to droop control in order to compensate for steady state errors. Fig. 3(a) demonstrates the conventional cascaded primary and secondary control as well as the required communication infrastructure. Compared to the conventional architecture, Fig. 3(b) shows the proposed communication-free control structure. This approach is realized by adjusting the local droop characteristic of each VSC. This adaptive droop configuration can be formulated as follows:

$$\omega_{ref} = \omega_{nom} + D_Q Q + \hat{D}_Q\frac{dQ^f}{dt}, \tag{13}$$

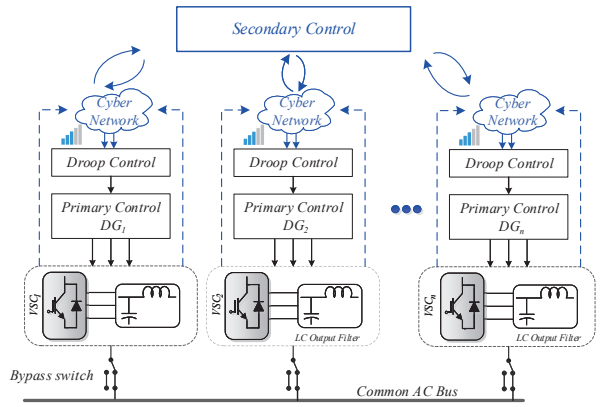

(a) Conventional centralized hierarchical control structure of microgrid

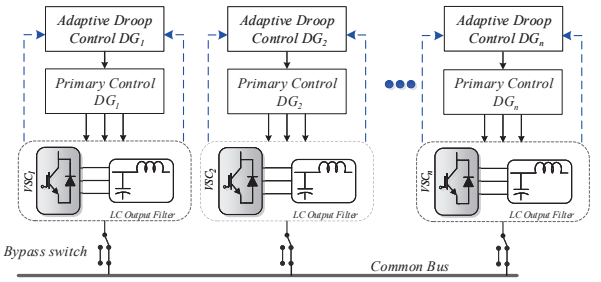

(b) Proposed communication free control structure of microgrid

Fig. 3. Comparison between conventional primary and secondary control architecture and the proposed communication-free control structure of the microgrid.

$$V_{ref} = V_{nom} - D_P P - \hat{D}_P \frac{dP^f}{dt}, \tag{14}$$

where, $\hat{D}_P$ and $\hat{D}_Q$ are the adaptive gains, and $\frac{dQ^f}{dt}$ and $\frac{dP^f}{dt}$ are the additional derivative terms of Q and P through a low pass filter, respectively. Thus, in order to have an acceptable time scale separation between the droop characteristic and adaptive term of active and reactive power the low pas filter with cutoff frequency ω_f can be applied as follows:

$$P^f = \frac{\omega_f}{s + \omega_f} P \tag{15}$$

$$Q^f = \frac{\omega_f}{s + \omega_f} Q \tag{16}$$

It worth to note that the resistive virtual impedance is implemented in the system. Although inductive virtual impedance is utilized in several studies, since resistive impedance value does not rely on the frequency, hence, has no effect on nonlinear load, its better to employ resistive impedance in the MG. Therefore, virtual impedance enforces the output impedance, seen by the VSC, to be purely resistive ($(\theta_i = 0)$).

The small signal equivalent around the operating point can be obtained as follows:

TABLE II. TEST SYSTEM PARAMETERS USED IN SIMULATIONS.

Parameter	Symbol	Value
DC Voltage	V_{dc}	$520\ V$
Nominal voltage amplitude	V_{nom}	$200\ V$
Nominal frequency	f_{nom}	$50\ Hz$
LC filter	$L_f,\ C_f$	$L_f = 2.4\ mH,\ C_f = 15\ \mu F$
Sampling time	T_s	$25\ \mu s$
Droop coefficients	$D_p,\ D_q$	$D_p = 0.005\ V/W,\ D_q = 0.002\ rad/sVar$
Line impedance	$R_l,\ L_l$	$R_l = 0.1\ \Omega,\ L_l = 2.4\ mH$
Virtual resistance	R_v	$2\ \Omega$

$$\Delta P(s) = \frac{G_p}{(1+\hat{D}_p G_p)s + D_p G_p} \Delta V_{nom} - \frac{G_p}{(1+\hat{D}_p G_p)s + D_p G_p} \Delta V_{MG}, \tag{17}$$

$$\Delta Q(s) = \frac{G_Q}{\hat{D}_Q G_Q s + (1 + D_Q G_Q)} \Delta \omega_{nom} + \frac{G_Q}{\hat{D}_Q G_Q s + (1 + D_Q G_Q)} \Delta \omega_{MG}, \tag{18}$$

where G_p and G_Q can be obtained from (10). As it can be seen from (17) and (18), the eigenvalue of the system around operating point can be achieved as follows:

$$\lambda P_0 = \frac{-D_p G_p}{1 + \hat{D}_p G_p}, \tag{19}$$

$$\lambda Q_0 = \frac{-(1 + D_q G_q)}{\hat{D}_q G_q}. \tag{20}$$

Consequently, by adjusting $\hat{D}_P$ and $\hat{D}_Q$ the desired dynamic performance of the system is achieved which after a transient not only keeps the power sharing, but also, the steady state errors of the frequency and voltage will be eliminated. Though, small oscillation in the steady state may be increased, due to derivative characteristics of the adaptive droop, but accurate adjusting of this term mitigates this drawback. MG network parameters and the linearization point should be considered in adaptive control law (13) to adjust of the adaptive terms accurately.

IV. SIMULATION RESULTS

In order to study the performance of the proposed control methodology, an autonomous MG is considered. The case study model is comprised of two VSCs connected to the common AC bus through dedicated LC filter and the power lines. The rated voltage and frequency are 200 V and 50 Hz, respectively. Other control and electrical parameters of the underlying case study are tabulated in details in Table II.

Performance of the proposed distributed control structure is evaluated under a frequency load change at t=30 ms in comparison with the conventional droop control. Figure 4(a) and (b) shows the active and reactive power sharing between two VSCs. As can be seen, after the load change at t=30 ms the

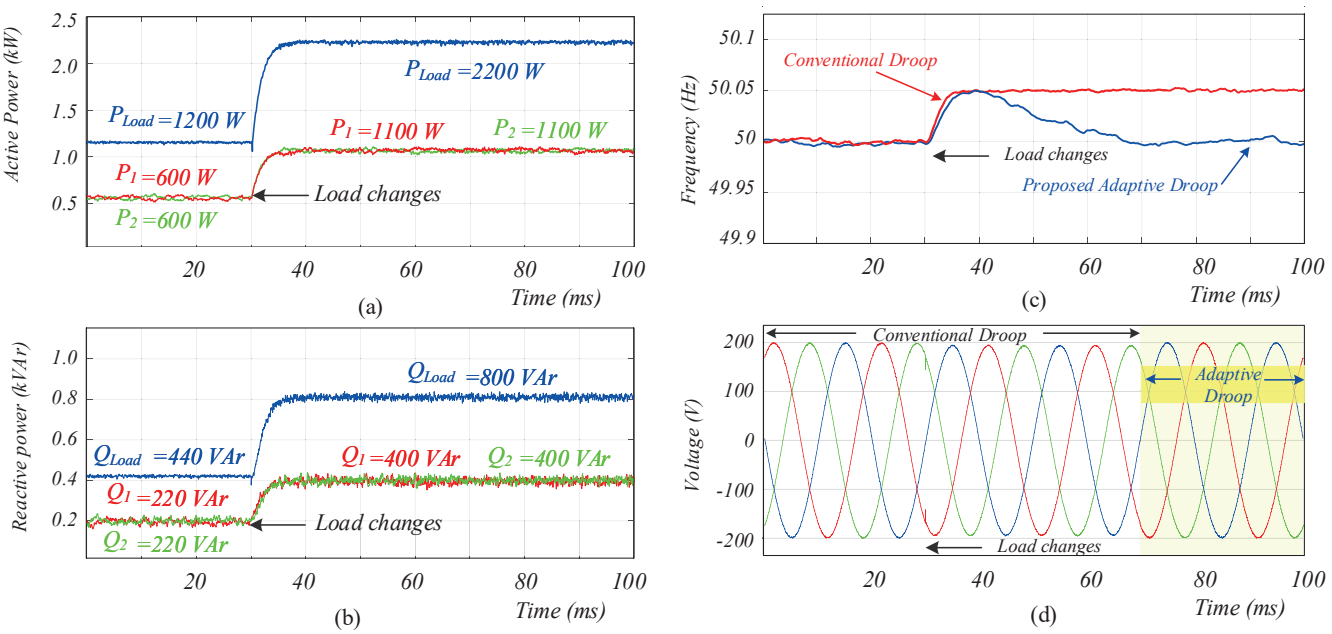

Fig. 4. Validation of the proposed control strategy under a load change. (a) Active power sharing between two VSCs. (b) Reactive power sharing between two VSCs. (c) Frequency restoration during a load change. (d) Voltage regulation performance.

active and reactive power output of the VSCs follow the load change accurately with super fast dynamic response. Worthing to note that the conventional cascaded control structure shares the power in the order of several seconds, while the proposed FCS-MPC based control structure shares the power in the order of 10 mili-seconds (see Fig. 16 in [19]). Figure 4 (c) and (d) shows a comprehensive comparison between the proposed adaptive droop control and conventional droop control. As can be seen from the Figure 4 (c) the conventional droop control has an steady state error, and a secondary controller is required to adjust the droop characteristics. However, the proposed adaptive droop compensates for the frequency deviation error caused by conventional droop with no need to the secondary control or communication network. Figure 4 (d) also shows the voltage compensation with the proposed adaptive droop implementation. Figure 4 also shows the supplementary term of adaptive droop control has no effect on the steady state performance of the MG. Therefore, based on the simulation results, the MG frequency and voltage maintained stable without any communication network infrastructure.

V. Conclusion

This paper proposed a communication-free control structure for the voltage and frequency restoration of the MG. An FCS-MPC is deployed at the primary control level of the hierarchical control structure to keep the frequency and voltage of the MG stable. Then, at the upper-level droop control and resistive virtual impedance is employed to share the power accurately and satisfy the control low. Finally, a new term of power derivative is supplemented to droop controller to adjust the droop characteristic and compensate for the voltage and frequency deviations in steady state. Simulation results for an autonomous MG showed that by applying the proposed control structure, not only the power sharing is carried on faster than the state of the arts, but also the MG frequency and voltage are restored with no need to communication infrastructure.

References

[1] Q. Shafiee, J. M. Guerrero, and J. C. Vasquez, "Distributed secondary control for islanded microgridsa novel approach," *IEEE Trans. Power Electron.*, vol. 29, no. 2, pp. 1018–1031, 2014.

[2] R. Heydari, T. Dragicevic, and F. Blaabjerg, "Coordinated operation of vscs controlled by mpc and cascaded linear controllers in power electronic based ac microgrid," in *2018 IEEE 19th Workshop on Control and Modeling for Power Electronics (COMPEL)*, pp. 1–4, IEEE, 2018.

[3] N. Bazmohammadi, A. Tahsiri, A. Anvari-Moghaddam, and J. M. Guerrero, "A hierarchical energy management strategy for interconnected microgrids considering uncertainty," *International Journal of Electrical Power & Energy Systems*, vol. 109, pp. 597–608, 2019.

[4] A. Anvari-Moghadam, Q. Shafiee, J. C. Vasquez, and J. M. Guerrero, "Optimal adaptive droop control for effective load sharing in ac microgrids," in *IECON 2016-42nd Annual Conference of the IEEE Industrial Electronics Society*, pp. 3872–3877, IEEE, 2016.

[5] A. Anvari-Moghaddam, J. M. Guerrero, J. C. Vasquez, H. Monsef, and A. Rahimi-Kian, "Efficient energy management for a grid-tied residential microgrid," *IET Generation, Transmission & Distribution*, vol. 11, no. 11, pp. 2752–2761, 2017.

[6] B. Shakerighadi, A. Anvari-Moghaddam, E. Ebrahimzadeh, F. Blaabjerg, and C. L. Bak, "A hierarchical game theoretical approach for energy management of electric vehicles and charging stations in smart grids," *Ieee Access*, vol. 6, pp. 67223–67234, 2018.

[7] M. Savaghebi, A. Jalilian, J. C. Vasquez, and J. M. Guerrero, "Secondary control for voltage quality enhancement in microgrids," *IEEE Trans. Smart Grid*, vol. 3, no. 4, pp. 1893–1902, 2012.

[8] T. Dragičević, R. Heydari, and F. Blaabjerg, "Super-high bandwidth secondary control of ac microgrids," in *2018 IEEE Applied Power Electronics Conference and Exposition (APEC)*, pp. 3036–3042, IEEE, 2018.

[9] A. Kaur, J. Kaushal, and P. Basak, "A review on microgrid central controller," *RENEW. SUST. ENERG. REV.*, vol. 55, pp. 338–345, 2016.

[10] Q. Shafiee, T. Dragicevic, J. C. Vasquez, J. M. Guerrero, C. Stefanovic, and P. Popovski, "A novel robust communication algorithm for distributed secondary control of islanded microgrids," in *Energy Conversion Congress and Exposition (ECCE), 2013 IEEE*, pp. 4609–4616, IEEE, 2013.

[11] J. W. Simpson-Porco, Q. Shafiee, F. Dörfler, J. C. Vasquez, J. M. Guerrero, and F. Bullo, "Secondary frequency and voltage control of islanded microgrids via distributed averaging.," *IEEE Trans. Ind. Electron.*, vol. 62, no. 11, pp. 7025–7038, 2015.

[12] R. Heyderi, A. Amiri, T. Dragicevic, P. Popovski, and F. Blaabjerg, "High bandwidth distributed secondary control with communication compensation in vsc-based microgrid," in *2018 20th European Conference on Power Electronics and Applications (EPE'18 ECCE Europe)*, pp. P–1, IEEE, 2018.

[13] R. Heydari, M. Gheisarnejad, M. H. Khooban, T. Dragicevic, and F. Blaabjerg, "Robust and fast voltage-source-converter (vsc) control for naval shipboard microgrids," *IEEE Trans. Power Electron.*, 2019.

[14] M. Castilla, A. Camacho, J. Miret, M. Velasco, and P. Marti, "Secondary control for inverter-based islanded microgrids with accurate active-power sharing under high load conditions," *IEEE Trans. Ind. Electron.*, 2018.

[15] J. M. Rey, P. Martí, M. Velasco, J. Miret, and M. Castilla, "Secondary switched control with no communications for islanded microgrids," *IEEE Trans. Ind. Electron.*, vol. 64, no. 11, pp. 8534–8545, 2017.

[16] Y. Khayat, M. Naderi, Q. Shafiee, M. Fathi, H. Bevrani, T. Dragicevic, and F. Blaabjerg, "Communication-less optimal frequency control of islanded microgrids," in *20th Europ. Conf. on Power Electron. Appl. (EPE'18 ECCE Europe)*, pp. P–1, IEEE, 2018.

[17] Y. Khayat, M. Naderi, Q. Shafiee, Y. Batmani, M. Fathi, J. M. Guerrero, and H. Bevrani, "Decentralized optimal frequency control in autonomous microgrids," *IEEE Transa. Power Syst. , DOI: 10.1109/TPWRS.2018.2889671.*, 2018.

[18] R. Heydari, T. Dragicevic, and F. Blaabjerg, "High-bandwidth secondary voltage and frequency control of vsc-based ac microgrid," *IEEE Transactions on Power Electronics*, 2019.

[19] Q. Shafiee, Č. Stefanović, T. Dragičević, P. Popovski, J. C. Vasquez, and J. M. Guerrero, "Robust networked control scheme for distributed secondary control of islanded microgrids," *IEEE Trans. Ind. Electron.*, vol. 61, no. 10, pp. 5363–5374, 2014.

[20] T. Dragicevic, M. Lu, and F. Blaabjerg, "Improved model predictive control for high voltage quality in ups applications," in *2017 IEEE Energy Conversion Congress and Exposition (ECCE)*, pp. 1–7, Sept 2017.

[21] X. Wang, Y. W. Li, F. Blaabjerg, and P. C. Loh, "Virtual-impedance-based control for voltage-source and current-source converters," *IEEE Trans. Power Electron*, vol. 30, no. 12, pp. 7019–7037, 2015.